PHYSICAL REVIEW B VOLUME 15, NUMBER 12 15 JUNE 1977

Oxygen adsorption on molybdenum studied by low-energy secondary-ion mass spectrometry and electron-induced desorption

P. H. Dawson
Division of Physics, National Research Council, Ottawa, Canada K1A OR6
(Received 28 December 1976)

The adsorption of oxygen on molybdenum in the monolayer region was studied using a combination of secondary-ion mass spectrometry (SIMS) at low primary energies and electron impact desorption. By examining the ion yields during adsorption and desorption at various temperatures, it was possible to identify two strongly bound states with activation energies for desorption of 120 and 107 kcal/mole. At room temperature, these β states are populated first and afterwards there are at least two α states which are simultaneously filled. The desorption energies for the α states were estimated to be about 37 kcal/mole. One α state gives rise to electron-induced desorption of O_e^+, the other does not. After only partial filling of the α states, a transformation of the state giving O_e^+ could be observed at quite low temperatures (>550°K). The rate of transformation was greater, the lower the degree of occupation of the α states. The β_1, β_2, and α states have quite different influences on the SIMS ion yields. The formation of the oxide produces characteristic changes in ion yields. Secondary-ion energies were also measured. The value of low-energy SIMS in characterizing different states of adsorption is demonstrated.

I. INTRODUCTION

Secondary-ion mass spectrometry (SIMS) is now widely used in materials analysis, but the technique is only at the stage of preliminary exploration concerning its application to the study of adsorbed layers.[1-9] "Static" SIMS, carried out under ultrahigh-vacuum conditions has given useful information about oxygen interactions with metals[2-4] after high oxygen exposures. Recently, the use of low primary-ion energies has allowed quantitative SIMS measurements in the monolayer adsorption region and the results can be correlated with those obtained using other surface spectroscopies such as Auger-electron (AES) and appearance-potential spectroscopy.[5-7] The adsorption of oxygen on aluminum[5] and titanium[7] has been studied in this way, but the work was limited to room temperature with the surfaces cleaned by ion bombardment and in some equilibrium state of damage. In this study of molybdenum, the target could be cleaned by heating to high temperatures and/or by ion bombardment, and the damage could be annealed out. Damage during the experiments should be quite low because of the low beam intensity.

Measurement of the secondary-ion yields during adsorption and desorption at various temperatures showed the existence of several different states of adsorption characterized by their activation energies for desorption. Each state has a characteristic influence on the SIMS yield patterns. The mechanisms of secondary-ion formation are not well understood; no theory exists at the present time which takes account of adsorbed layers. However, the large qualitative differences between yield patterns for different states of adsorption must be related to the oxygen adatom positions, and their bonding to the molybdenum substrate. This is the first detailed correlation of changes in SIMS yields with specific states of adsorption. The very complexity of the SIMS spectra presents the possibility of a powerful diagnostic technique if the controlling factors can be elucidated. The accumulation of data on different binding states of various adsorption systems and their correlation with other surface measurements is an important first step.

Oxygen adsorption on molybdenum has previously been examined using electron-induced desorption (EID).[10-12] The results reported here are in general agreement with the work of Redhead,[10] although there are differences of interpretation based on the simultaneous SIMS observations. The Mo-O_2 system has also been examined previously using low-energy-electron diffraction (LEED),[13-16] AES,[16] work-function changes,[16] and electron-energy-loss spectroscopy.[16,17] Where possible, comparisons are made between the SIMS results and the previous measurements.

Energy distributions for secondary ions produced by SIMS and EID are also reported. These may be important in the development and testing of models for secondary-ion formation.

II. EXPERIMENTAL PROCEDURES

The experimental apparatus and its performance have been described in detail elsewhere.[6] Its important characteristics are as follows. The apparatus (Fig. 1) operates under ultrahigh-vacuum conditions. The primary beam of argon ions is mass analyzed. The primary energy is only 500 eV and the primary ion current, about 1.5×10^{-9} A.

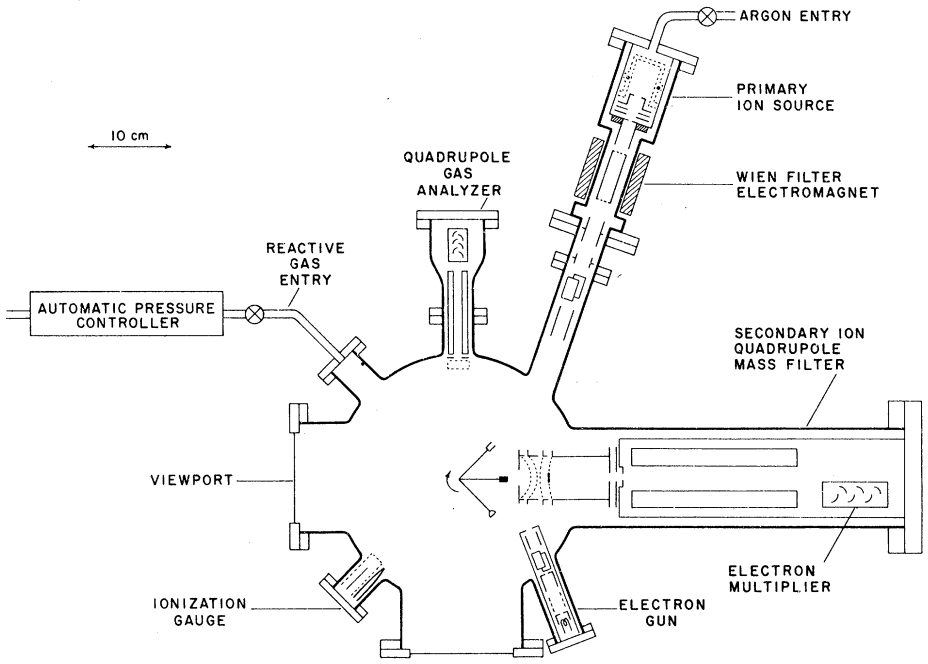

FIG. 1. Schematic view of the apparatus.

During the operation of the ion gun, the argon pressure at the target is less than 10^{-9} Torr so that the pressure of reactive gas also admitted can be accurately measured and controlled. The gas purity can be monitored with a quadrupole residual gas analyzer. The electron bombardment of the target (EID) was carried out using a beam of 200-eV energy and approximately 5×10^{-7}-A intensity. Secondary ions were collected from a large area of the target and from a large solid angle by a multigridded electrode system specially designed[18] to match the acceptance characteristics of a large-aperture quadrupole. The quadrupole was also fitted with a special field modifying entrance aperture.[19] The gridded electrode system can be used to perform secondary-ion energy analyses[6] and the central stop also serves to prevent any direct passage of neutral sputtered particles into the quadrupole and the detector. By maintaining the target a few volts positive with respect to the quadrupole axis, an operating region can be found where the differences in secondary-ion energy distributions (see below) and/or changes in target work function do not have a major influence on the ratios of different ions observed. That is, velocity discrimination effects of the quadrupole analyzer[20] are minimized. However, as in all mass spectrometric measurements, the observed "patterns" in the spectra are functions of the particular instrument and its operational setting (such as the dc/rf ratio).

The target was a polycrystalline molybdenum ribbon of cross section 0.005×0.2 cm^2 and about 4 cm long. It was bent so that only the central portion 0.4 cm long served as a source of secondary ions. The ribbon was heated electrically. Temperatures were determined using a Pt–Pt+10-at.%-Rh thermocouple which was calibrated with an optical pyrometer at the higher temperatures. At the lower temperatures, the filament leads do influence the observed temperatures and cause some drift of ribbon temperature as they heat or cool. This introduces a larger uncertainty in measurements made below 750 °K.

III. RESULTS

The SIMS and EID measurements reveal a complex picture of the adsorption process involving several states of adsorption of different binding energies. The results will be presented in several subsections grouped according to the temperature at which the adsorption was allowed to take place. The subsequent observations of desorption or other thermally induced changes are given in these same sections. Destruction of the adsorbed layer by sputtering is described later together with measurements of secondary-ion energy distributions.

The molybdenum target was cleaned by a combination of ion bombardment, heating in vacuum at temperatures of up to 1900 °K, and treatment with oxygen. The impurity peaks normally seen with great sensitivity in SIMS measurements on metals at room temperature (e.g., Na^+, K^+, etc.) were completely eliminated and the target reached a steady condition reproducible after flashing at high temperatures.

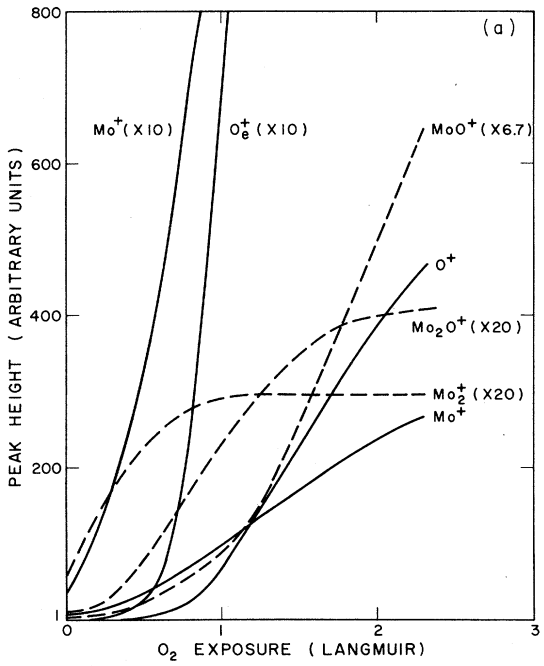

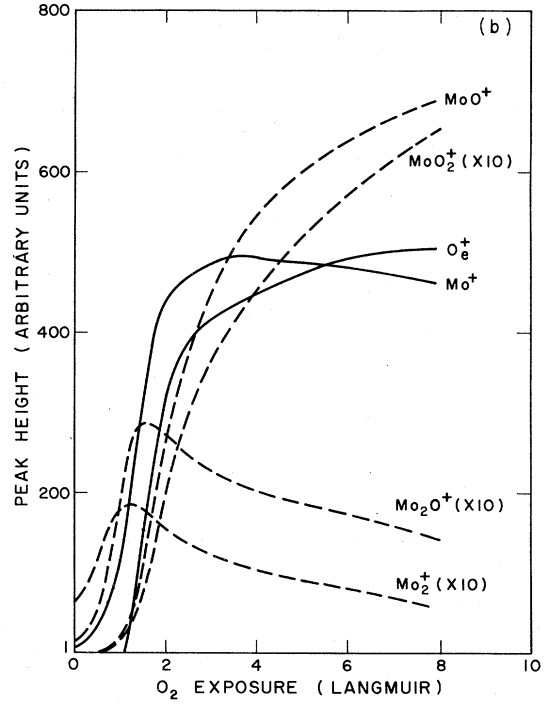

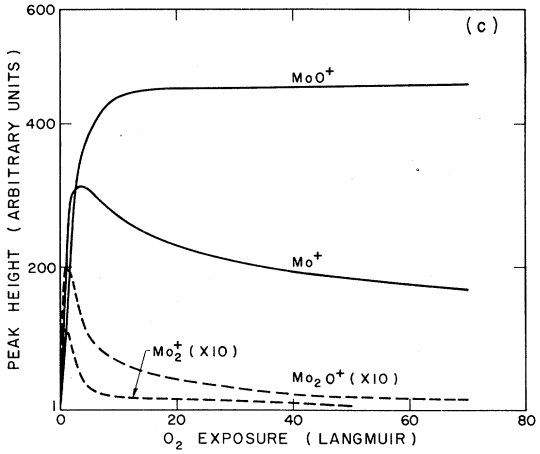

FIG. 2. Changes in SIMS and EID ion yields during the exposure of molybdenum to oxygen at room temperature after first cleaning by heating above 1900 °K. (a) 0–2-L region; oxygen pressure 5.6×10^{-10} Torr; (b) 0–8-L region; oxygen pressure 1×10^{-8} Torr; (c) 0–60-L region; oxygen pressure 2.1×10^{-8} Torr.

A. Adsorption at 300 °K

1. Yield changes on adsorption

Unless otherwise stated, the filament was outgassed at about 1900 °K before each set of measurements. In order that the changes in ion yields can be seen in detail, the results for room-temperature adsorption are presented on three different exposure scales in Figs. 2(a)–2(c). The argon ion current was about 2.5 times higher in these illustrations than in the subsequent measurements, but this has little influence on the course of events. At first sight the shape of the yield variation for Mo^+ and MoO^+ at lower exposures differs from those found in earlier work on other metals, such as Al and Ti. For these metals, changes in yield were found to be linear at low coverages. However, the curves of Fig. 2 are actually composed of contributions from several different states of adsorption which become occupied after different exposures. This will become evident when thermally induced changes in the adsorbed layer are considered. The decline in metal ion yield, Mo^+, shown in Fig. 2(c) at high exposures has previously been associated with the beginnings of oxide formation. Another notable feature in Fig. 2(a) is the delay before the appearance of O_e^+. (The suffix e is used to indicate electron-induced desorption.) This was previously reported by Redhead in his early EID studies.[10] He identified at least two states of adsorption occurring consecutively which he labelled states 1 and 2. Here we will use the designation of two groups of states, β and α. The α states adsorb subsequent to the

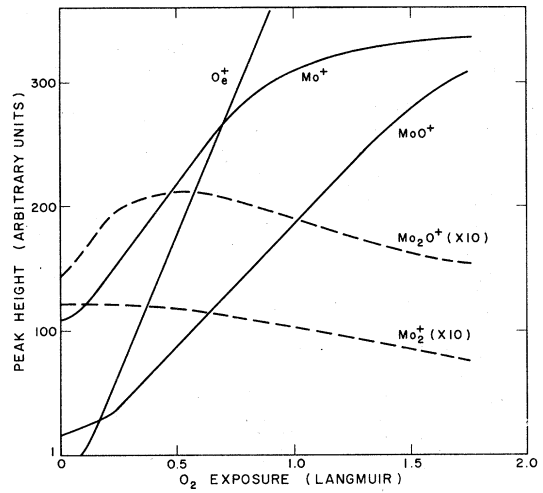

FIG. 3. Changes in ion yields with oxygen exposure at room temperature after first partially desorbing adsorbed oxygen at 1250 °K.

(partial) filling of the β states and are less strongly bound. An α state is the source of the O_e^+ emission. The α states are lost on heating to 1250 °K in vacuum. However, on cooling to room temperature and reexposing to oxygen, there is an almost immediate increase in the O_e^+ accompanied by the related changes in the other ion yields, as shown in Fig. 3.

The delay time in the formation of the O_e^+ yielding state was investigated in more detail at various oxygen pressures. The results are shown in Fig. 4. Within the limits of accuracy of the pressure measurement, the delay time δ is inversely proportional to the oxygen pressure and the slope of the linear portion is proportional to the oxygen pressure. A curve of similar slope for a given pressure, but with zero delay time, was found if the filament had been heated to only 1250 °K instead of 1900 °K after previous oxidation. Note that the growth of O_e^+ is more gradual at low coverages and near saturation when the oxygen pressure is low.

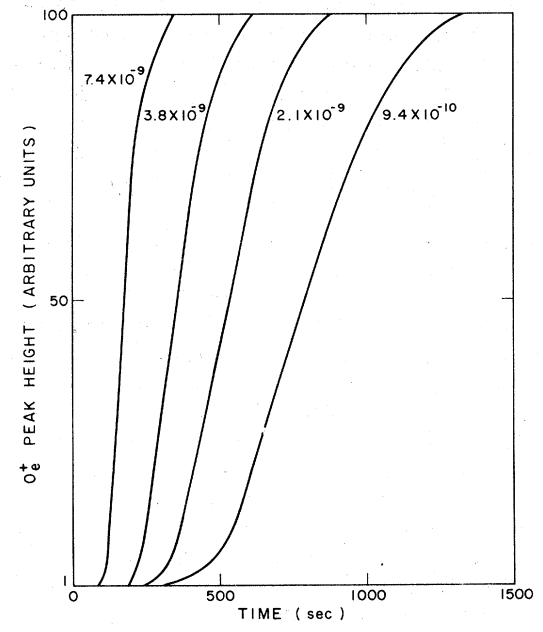

FIG. 4. Changes in O_e^+ peak height with time of exposure at room temperature at various oxygen pressures (given in Torr) after first heating at 1900 °K.

2. *Thermally induced changes after 300 °K adsorption*

It is simpler to consider first the most highly oxidized condition and then to progress to lower oxygen coverages where the thermally induced changes are more complex. Figures 5(a) and 5(b) show semilog plots of the variations of O_e^+ and MoO^+ on heating to 1020 °K after various degrees

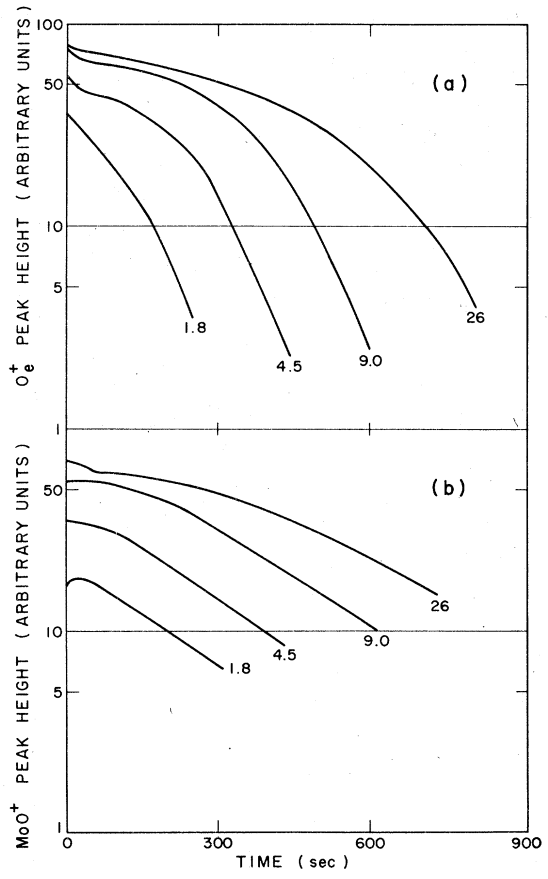

FIG. 5. (a) Changes in O_e^+ peak height on heating to 1020 °K after different degrees of oxygen exposure of the target at room temperature. The oxygen exposures are given in langmuir. (b) Corresponding changes in MoO^+ yields.

of oxygen exposure at 300 °K. The curves yield the kind of exponential decline that might be expected for a loss process from a monolayer involving an activation energy barrier, but there is an initial delay depending upon the extent of exposure or on what has been identified in Fig. 2(c) with the extent of oxide formation. Figure 6 illustrates the variations that are found in the other ion yields. The delay before the rapid decline in O_e^+ and MoO^+ is associated with the increase of Mo_2O^+ and Mo_2^+.

The O_e^+ ion was monitored in order to examine the influence of temperature on the rate of loss after a fixed room temperature exposure of about 2 langmuir (1 L = 10^{-6} Torr sec). The results are shown in Fig. 7. The delay is shorter at higher temperatures and the subsequent rate of decline is greater.

The measurements just described evidently relate to the loss of the oxide and the loss of the α states. The loss of the β states on heating to higher temperatures is described below since the β states can equally well be formed by adsorption at elevated temperatures.

A different phenomenon was observed when the α states were only partially filled. This is illustrated in Fig. 8. Adsorption was allowed to occur by oxygen exposure at 300 °K until the O_e^+ signal reached about one third of its saturation level. Heating at 1040 °K, in contrast with Fig. 5, produced an extremely rapid and marked decrease in O_e^+, but only small changes in the SIMS peaks. After the precipitous drop, O_e^+ continued to decline further in the expected exponential fashion. As shown in the figure, repeating the adsorption and heating cycle (with no intermediate outgassing at higher temperatures) gave different results. The depletion of the O_e^+ producing state was investigated at lower temperatures. Figure 9 shows cycles for adsorption at 300 °K followed by heating at 640 °K. The rate of decrease of O_e^+ was found to depend both upon the temperature and on the degree of filling of the state. Figure 10 compares the decrease of O_e^+ at two different temperatures, 720

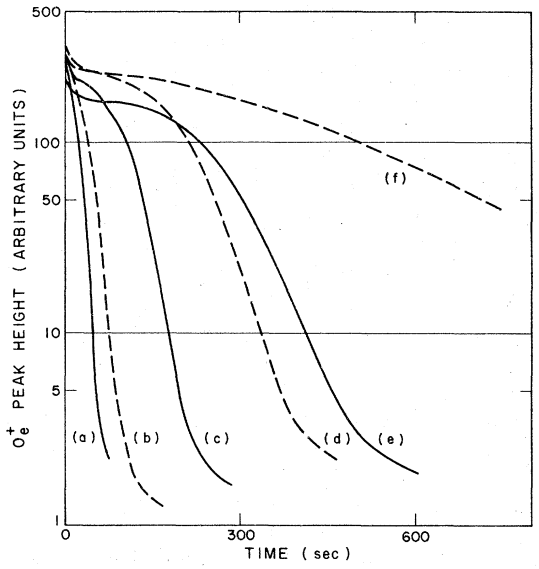

FIG. 7. Decline in O_e^+ on heating to various temperatures after room-temperature exposure to 2 L of oxygen. (a) 1235 °K, (b) 1190 °K, (c) 1145 °K, (d) 1115 °K, (e) 1070 °K, (f) 1010 °K.

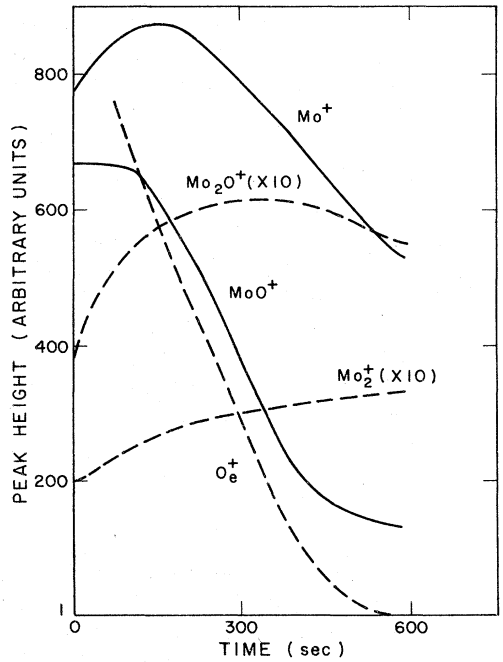

FIG. 6. Variations in sceondary-ion yields on heating to 1020 °K after oxygen exposure at room temperature.

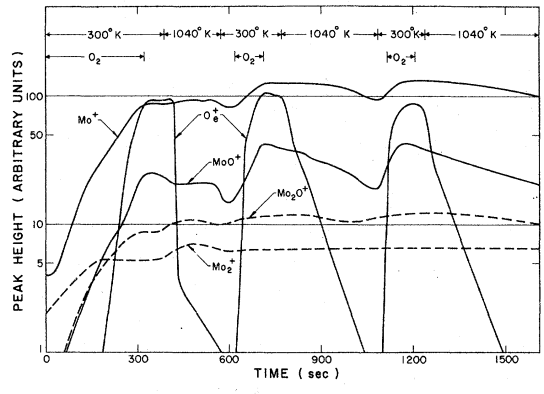

FIG. 8. Oxygen exposure at 300 °K until O_e^+ has reached about $\frac{1}{3}$ of its saturation level followed by heating at 1040 °K and repeated cycles of this treatment.

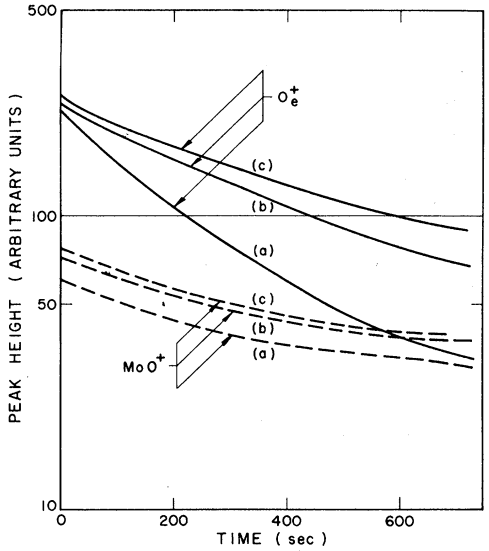

FIG. 9. Observations on O_e^+ and MoO^+ during three cycles of heating at 640 °K following adsorption at 300 °K carried out in the sequence (a)–(c).

and 580 °K, starting with the same initial signal. Figure 11 shows a comparison for different initial levels of O_e^+ and a fixed heating temperature of 640 °K.

B. Adsorption at 640 °K

After cleaning by heating to 1900 °K, the adsorption of oxygen at 640 °K, produced by exposure at a pressure of 5×10^{-9} Torr, caused the yield

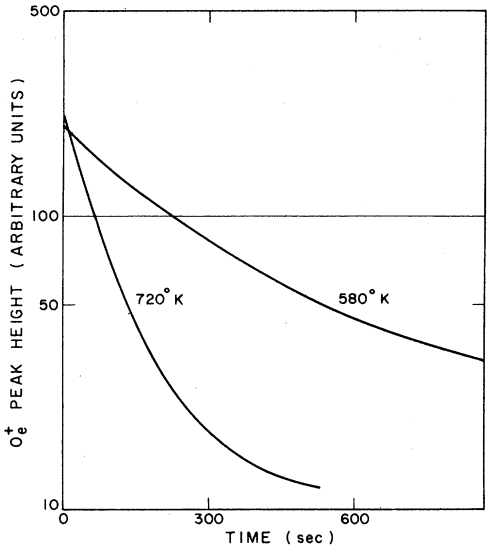

FIG. 10. Decline of the O_e^+ signal on heating to 580 and 720 °K after filling to the same initial condition by adsorption at 300 °K.

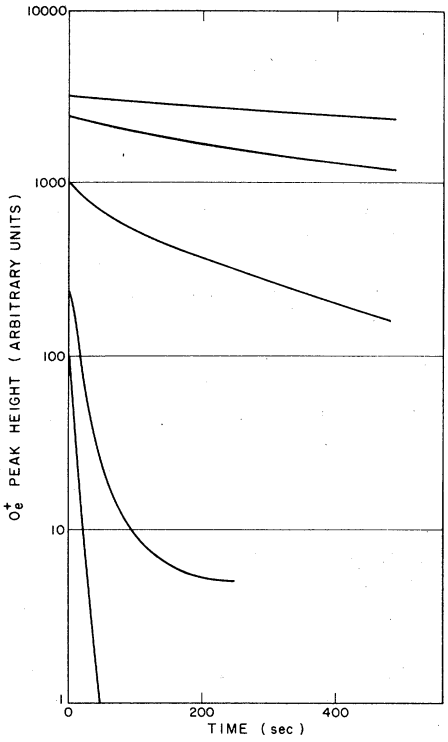

FIG. 11. Decline of the O_e^+ signal on heating to 640 °K after adsorption at 300 °K to different degrees of saturation.

changes shown in Fig. 12(b). Figure 12(a) gives the curves for room-temperature adsorption taken under similar conditions. After only partial filling of the α states by adsorption at 640 °K, no decline in O_e^+ was observed when the oxygen exposure was terminated (in contrast with the phenomenon described above following room-temperature adsorption).

C. Adsorption at 1250 °K

As described earlier, the α states are removed by heating above about 1000 °K. Exposure of the cleaned surface to oxygen at 1250 °K forms only β states. The changes in ion yields when the oxygen pressure was 5×10^{-9} Torr are shown in Fig. 12(c). Subsequent changes on heating first to 1600 °K and then to 1880 °K are shown in Fig. 13. There appear to be at least two β states with different SIMS characteristics.

D. Adsorption at 1600 °K

The cleaned target was heated at 1600 °K and exposed to oxygen at a pressure of 6.6×10^{-9} Torr with the results given in Fig. 14. After the oxygen exposure had been terminated, heating to 1780 °K reversed the changes in ion yields.

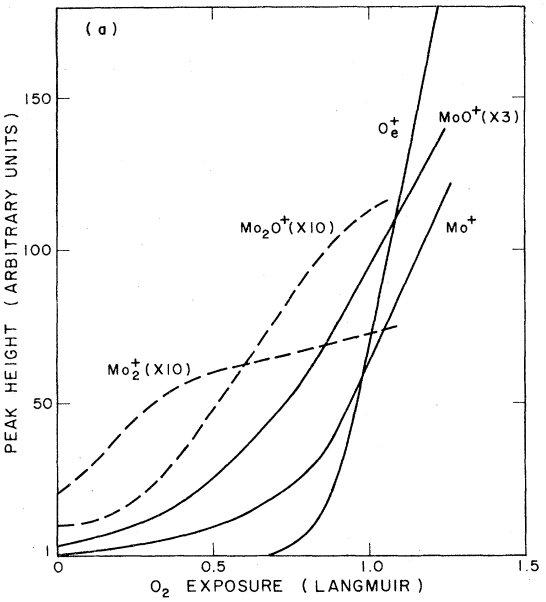

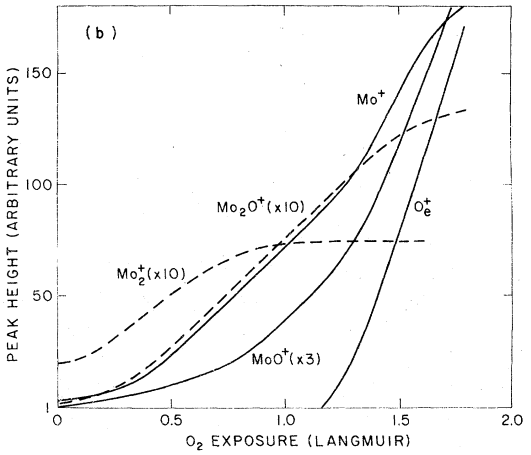

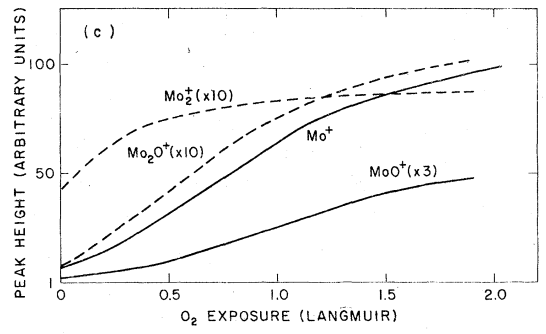

FIG. 12. Changes in ion yields as a function of oxygen exposure at various target temperatures when the oxygen pressure was 5×10^{-9} Torr. (a) 300 °K, (b) 640 °K, (c) 1250 °K.

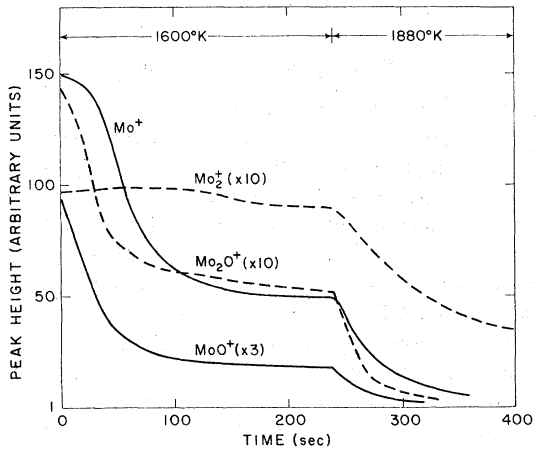

FIG. 13. Changes in ion yields on heating successively to 1600 and 1880 °K after oxygen adsorption at 1250 °K.

A curious phenomenon was observed with the O_e^+ signal at high temperatures. At 1200 °K, the O_e^+ signal was less than 0.5% of that observed with full occupation of the α states. At higher temperatures, when heating in vacuum, the O_e^+ signal increased, although rapidly reaching a steady level at each temperature. At 1750 °K it had increased to about 5%. This phenomenon persisted even after a great deal of outgassing of the target. A similar effect was evident in Redhead's earlier work.[21] The O_e^+ signal was in no way related to the changes in other ion yields in the temperature range of 1200–1750 °K described above. The O_e^+ ion energy distribution was quite similar (see below) to that found when the α states were present at lower temperatures. The origin of this signal is not known. It may be related to impurity diffusion to the surface, providing some small fraction of the surface with a high probability of O_e^+ formation.

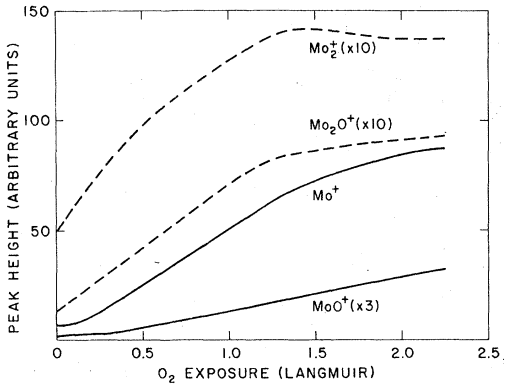

FIG. 14. Changes in ion yields as a function of oxygen exposure with the molybdenum at 1600 °K.

E. Sputtering of the adsorbed layer

The changes in ion yield during the adsorption of oxygen could be reversed by continuous sputtering at room temperature in the absence of oxygen. Figure 15 shows some data taken after room-temperature exposure of the target to about 9 L of oxygen. The primary-ion current was about 2.5 times higher than that used in the adsorption experiments described above. There is a very rapid reversal of those changes associated earlier with oxide formation. This has also been seen in the work with aluminum[5] and titanium[7] and in the work of Benninghoven.[1-4] The exponential decays in Fig. 15 can be interpreted[1,5] in terms of cross sections for desorption and/or destruction Q since for monolayer kinetics the characteristic decay time τ is given by $\tau = 1/\nu Q$, where ν is the intensity of bombardment of the primary beam. The cross section indicated from the Mo^+ curve would be about 4.4×10^{-15} cm^2 and that from the MoO^+ and MoO_2^+ about 7.7×10^{-15} cm^2.

F. Secondary-ion energies

The procedure for measuring secondary-ion energies has been described in detail previously.

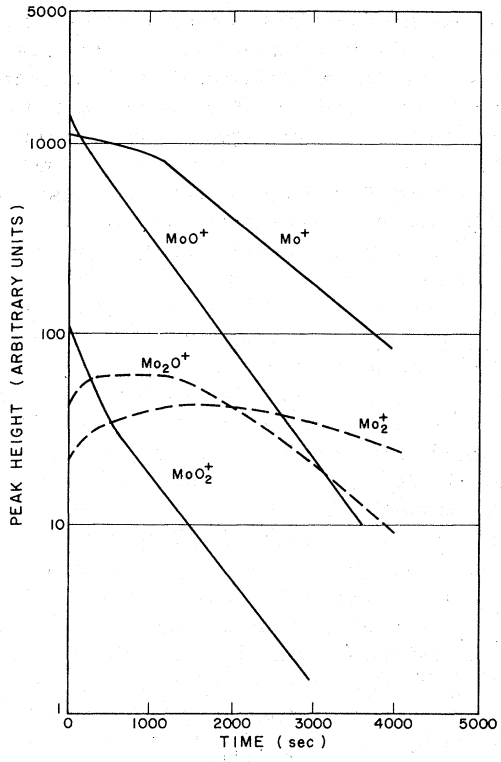

FIG. 15. Changes of ion yields with the time of sputtering after exposure of the surface to 9 L of oxygen. The Ar^+ primary ion current was 3.5×10^{-9} A.

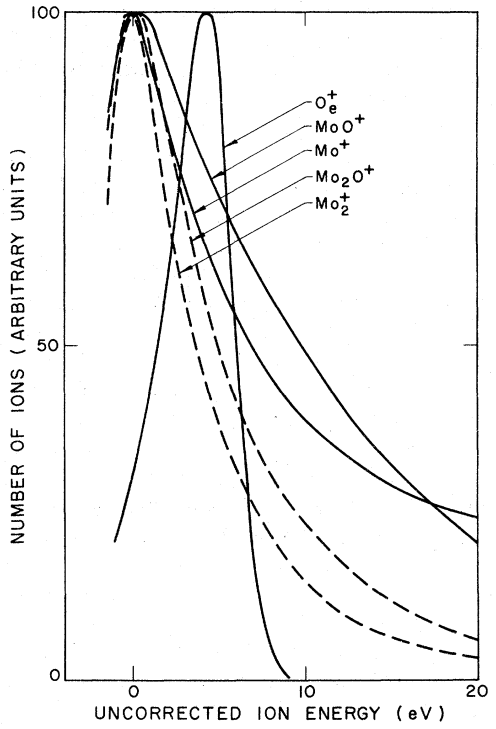

FIG. 16. Secondary-ion energy distributions after oxygen adsorption on the molybdenum surface. The energy scale is uncorrected for contact potential difference.

Figure 16 shows measurements on O_e^+, Mo^+, MoO^+, Mo_2^+, and Mo_2O^+ taken at room temperature after exposing the target to about 3.5 L of oxygen. The target was then heated to 1250 °K, and maintained at that temperature while the energy distributions were remeasured. This ensures the absence of the α adsorbed states. All the curves (O_e^+ being absent, of course) were identical in shape within the experimental error, but shifted about 0.5 eV towards higher apparent energies. This would correspond to a decrease in the work function of the target surface. The experimental errors in measuring energy distributions of Mo^+ from the cleaned surface at either room temperature or at 1900 °K were large because of the low secondary-ion yields. However, the distributions were generally similar to those described above.

The small O_e^+ signal appearing at high temperatures had a very similar energy distribution to that shown above except for a slight broadening.

IV. DISCUSSION

A. Different states of adsorption

In the preceding section the discussion of the data in terms of two regimes involving adsorption

and oxidation has already been anticipated. The adsorption regime is further subdivided into two groups of states, α and β, of quite different binding energies, each of which is made up of at least two states of adsorption.

Referring to Figs. 2 and 12, at room temperature one can divide the oxidation into three stages with some overlap between the stages as follows: (a) 0–1.5 L exposure, β states, relatively small changes in ion yields; (b) 0.75–3 L, α states, including a state producing O_e^+ and large increases in secondary-ion yields; (c) > 3 L, oxide regime, decline of Mo^+ and saturation of MoO^+. The association of a decline in metal atom yield (Mo^+), with the formation of an oxide regime has previously been suggested in SIMS measurements during oxygen adsorption on both aluminum[5] and titanium[7] even though the mechanisms of adsorption appear to be quite different in all three cases. Independent evidence obtained using other techniques on oxide formation was available for these metals. For Mo(100), recent work by Riwan *et al.* using AES, LEED, and work-function measurements has also identified three stages in the interaction with oxygen at room temperature. From 0–1 L exposure, there is a $c(2\times 2)$ structure associated with a decrease in work function. In the second stage (1–3.5 L) a sharp initial increase in work function was observed, followed by a plateau. Above 3.4 L, the work function increased slowly to saturation along with the appearance of LEED patterns attributed to surface oxides. Supporting evidence for the first stage comes from the electron-loss spectroscopic measurements of Ballu and Lecante.[17] It is interesting to note that the difference in work function at the end of the first stage compared to the end of the second stage also appears to be reflected in the secondary-ion energy distribution measurements described above. The existence of the two groups of adsorption states was evident in the early work of Redhead[10] on EID and was confirmed by Lichtman and Kirst[11] and by Klopfer[12] although the latter did not determine the binding energies of the states of adsorption.

Benninghoven[1] has also reported some SIMS measurements on the oxidation of molybdenum at room temperature with an unannealed target and a primary-ion energy of 3 keV. He found a large increase in Mo^+ and MoO^+ yields only after exposures of about 50 L. Clearly, this phenomenon is not the same as the examination of the monolayer region reported here.

Provided no changes occur in surface composition, SIMS yields (and secondary-ion energy distributions) appear relatively insensitive to temperature changes. The yields of both Mo^+ and Mo_2^+ were found to increase slowly with the target temperature. In an experiment where the molybdenum was outgassed at 2000 °K before each measurement at a lower temperature in order to try to ensure similar surface conditions, the yields were found to decrease approximately exponentially with $1/T$, but with an apparent activation energy of less than 1.5 kcal/mole. SIMS therefore provides a technique for detailed examination of the surface itself during thermal desorption measurements. Thus, measurements at high temperatures during adsorption and desorption clearly demonstrate the presence of at least two different β states of different binding energies. Allowing for probable variations in sticking probability with temperature, the similarity of the yield changes observed in the initial stages of adsorption at room temperature [Fig. 12(a)], at 640 °K [Fig. 12(b)], and 1250 °K [Fig. 12(c)] suggest that the observations of adsorption/desorption characteristics at high temperatures are relevant to room-temperature adsorption in this particular case. The heats of adsorption of the β_1 and β_2 states can be estimated from observations of the type illustrated in Fig. 14. Allowing for the residual signals, the curves approximately match those for a first-order desorption. For strongly bound states a preexponential factor of $\tau_0 = 10^{-13}$ sec can be assumed and this would indicate activation energies for desorption of 120 and 107 kcal/mole. These are in agreement with the 110 kcal/mole found by Redhead[10] from the observation of pressure changes.

B. α states

Analysis of the α states is more complex. Both during adsorption and desorption measurements (Figs. 2, 3, and 6) the O_e^+ yield variations are associated with characteristically large changes in the SIMS yields, especially Mo^+ and MoO^+. It is evident that the α states are only observed after a substantial occupation of the β states. However, when the α state is only partially occupied, heating to quite low temperatures (e.g., > 550 °K) leads to a rapid decrease in O_e^+ with only a small decrease in MoO^+ (Fig. 8) and very small changes in other ion yields. This is discussed in some detail later. The observations can be explained by postulating two types of α state, one which gives rise to O_e^+, and occupies only a fraction of the surface and one which does not produce O_e^+. These states will be designated α_2 and α_1, respectively. They cannot be distinguished on energetic grounds in these experiments. In the desorption experiments from the filled α states (Fig. 6), the changes are not exactly the reverse of those during adsorption (Fig. 3) especially for Mo^+. This may indicate that there is a partial transformation of the α states to

some other adsorbed state rather than *total* desorption. The O_e^+ variations on heating to >1000 °K can be readily represented by a first-order process (Fig. 7), except for an initial delay which decreases at higher temperatures. The delay also varies with the degree of oxygen exposure (Fig. 5) for a fixed desorption temperature. During the delay, the Mo^+, Mo_2^+, and Mo_2O^+ peaks increase, indicating loss of the oxide regime from the surface. The structures responsible for the O_e^+ production (and the associated MoO^+) are "locked" in place by the presence of the oxide regime. At high levels of oxidation, the transition from one regime to the other becomes less clear-cut (Fig. 5). At lower exposures, the delay is approximately proportional to the exposure.

The inverse slopes of the decay curves of Fig. 7 are plotted versus $10^4/T$ in Fig. 17. They indicate a desorption rate given by

$$R = 10^{5.7} e^{-37\,000/RT}.$$

The delay times in Fig. 7 also vary approximately exponentially with $1/T$, especially at the higher temperatures, and are consistent with an activation energy of the same order of magnitude, suggesting perhaps that loss of the oxide regime involves a similar desorption process to loss of the α state. Redhead[10] reported a value of 60 kcal/mole for the heat of adsorption of the more weakly bound state but he arrived at this value on the basis of a fit to second-order kinetics when the coverage θ was less than 0.3. The more detailed data presented here are in conflict with this assumption. It is possible that Redhead's measurements were complicated by the presence of the phenomenon of the decay of O_e^+ from the partially filled state (Fig. 10) which does resemble a second-order process. Low preexponential factors like the one found here have previously been observed for various weakly bound adsorbed species on metal surfaces.[22]

The most complex kinetic process observed here was the rapid disappearance of the O_e^+ signal from the partially filled α state at quite low temperatures. Unlike the higher temperature loss described above, which is probably largely associated with desorption, the cycles of repeated heating and adsorption produce a change in the surface (Figs. 8 and 11). The phenomenon only occurred when heating to greater than about 500 °K after adsorption at room temperature. Exposure of the surface directly at 640 °K [Fig. 12(b)] gave a stable adsorbed state when the oxygen flow was terminated. This suggests that the change in O_e^+ arises from a rearrangement of the α_2 state formed at room temperature as the temperature is raised. However, this rearrangement only occurs if the adsorption states are not fully occupied, and occurs more rapidly the less the degree of occupation (Fig. 11). The process which affects the transformation requires only a small activation energy (Fig. 10). The final state depends on the past history of the surface (Figs. 8 and 9), on the degree of saturation of the α states, and on the temperature. The kinetics of the O_e^+ loss (Fig. 10 and 11) at any particular temperature and degree of α coverage (θ_α), resemble those for a second-order process. However, the variations with θ_α and particularly the variations in the "final" coverage are difficult to reconcile with such a simple process. A more likely explanation is that the process is an equilibration. The α_2 state interacts, for example, with a vacancy in the oxygen coverage to give a thermodynamically more stable state. This would lead to a high relative-loss rate at low coverage (high concentration of vacant sites) and zero loss rate at complete coverage (zero concentration of vacant sites). Reversibility of the process has to be assumed in order to account for the different final concentrations for different temperatures with a given θ_α (Fig. 10). The activation energy for the forward process (O_e^+ loss) might then be associated with some process of surface diffusion and rearrangement. The activation energy can be estimated from the initial slopes in Fig.

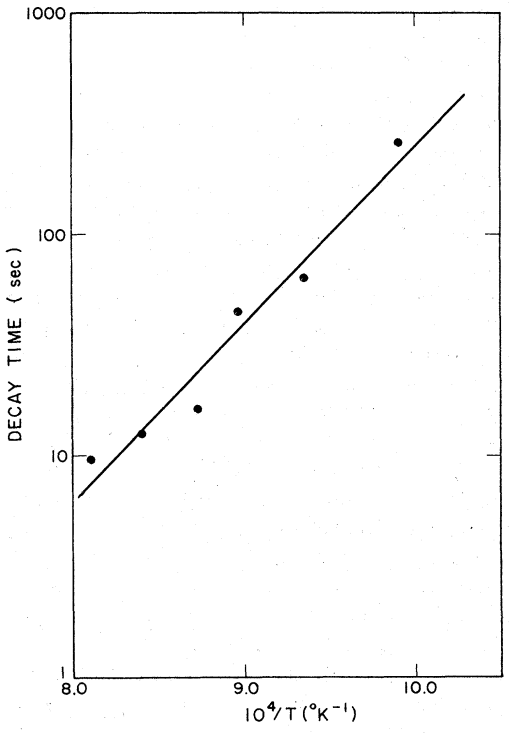

FIG. 17. The decay times derived from Fig. 7 plotted vs $1/T$.

10, since it is evident from the final concentration that the "back reaction" is initially quite small. The activation energy is only about 7 kcal/mole.

At low θ_α the exponential decay times (τ) are approximately proportional to θ_α as would be expected, but the times become even greater once $\theta_0 > \frac{1}{3}$. It would only be possible to fit the experimental curves to a detailed theoretical model if the relative populations of the states involved could be independently determined. Attempts to directly verify the occurrence of a "back reaction" by adsorbing at one temperature and then cooling the target were not successful. Transformations occurring at temperatures above 350 °K have also been observed in LEED studies of O_2 on Mo(100).[16]

C. Rates of coverage

Previous adsorption studies using SIMS on apparently simpler systems[5,7,23] have suggested that the changes in yield of the major ionic components (especially the metal ions M^+) are linear at low coverage. This feature is confirmed in the present work for each of the states of adsorption. The yield-versus-exposure curves can then be interpreted in terms of the initial rates of coverage of each adsorbed state assuming that saturation correponds to full coverage. From Fig. 14, for example, the Mo^+ curve would indicate an initial rate of coverage for the β_2 state of about 1 monolayer per 6×10^{14} collisions/cm^2 at 1600 °K. If the monolayer coverage, or more correctly, the saturation coverage,was known, it would be possible to calculate the sticking probability. Other initial rates of coverage for the β states were as follows: 1250 °K ($\beta_1 + \beta_2$), 6.3×10^{14} collisions/cm^2 monolayer; 640 °K ($\beta_1 + \beta_2$), 4×10^{14} collisions/cm^2 monolayer; 300 °K ($\beta_1 + \beta_2$), 3.3×10^{14} collisions/cm^2 monolayer. A certain degree of randomness in the process of filling the α_2 state is indicated in Fig. 4; the curves are less linear at lower pressures and there is more overlap with the β states. From Fig. 3, the initial coverage rate at 300 °K for the α states is also about 3.3×10^{14} collisions/cm^2 layer.

Using AES measurements on Mo(100), Riwan *et al.*[16] find a total coverage of 15×10^{14} *atoms*/cm^2 after 12 L exposure. The initial stage of oxidation (as described above) involved a coverage of 5×10^{14} atoms/cm^2 ($\theta = \frac{1}{2}$). The initial sticking coefficient was 0.5 and was almost constant throughout the first stage of adsorption. The constancy of the sticking probability with coverage despite the transition from a filling of β states to filling of α states suggests the possibility of a common precursor which is mobile when the β states are not fully occupied. In principle, the variation in sticking probability with coverage might be determined from the SIMS yield curves if the effects of coverage remain linear at high coverage.

D. SIMS yield characteristics

Implicit in the discussion of the SIMS results so far is that separate states of adsorption can be characterized by "fingerprints" of changes in ion yields and that these general characteristics are retained at different temperatures. The experimental data lend considerable support to this assumption. The question arises of how to represent these spectral characteristics. For example, since the α states are never present in the absence of β states, is it sufficient to present the overall spectrum as in Fig. 2 *et seq.*, or is it possible to decompose the spectrum into contributions due to the different adsorbed states? Such an analysis might be useful in deciphering information on adatom bonding or locations and would be important in trying to develop theroretical models for the dependence of SIMS yields on adsorption. The most informative presentation would be as the rate of change of ion yields per degree of occupation of each state. Of course, as in all mass spectrometric cracking patterns, the exact pattern depends upon the instrument characteristics. However, relative comparisons may be useful. Figure 18 compares the changes in yield observed for the various states of adsorption under similar instrument conditions. The overlap of the occupation of the various states and the occurrence of the oxide regime prevents a more accurate comparison.

The increase in the yield of metal ions (Mo^+) with adsorption of some gases has been observed many times before. It is presumably associated with a change in the ratio of ions to neutrals emitted in the sputtering process and might be related to changes in the probability of electron tunnelling into the vacuum.[7] The strongly adsorbed β_2 state increases all the ion yields substantially but for Mo_2^+ the relative increase is much smaller than for the other ions. This suggests an interference by the adsorbed oxygen with the probability of emission of the Mo_2 cluster.[5,7] The β_1 adsorption continues to increase all the ion yields except Mo_2^+ which remains almost constant. This provides a clear distinction between the two β states. It has been suggested from LEED and work-function measurements that on Mo(100),[16] even at room temperature, the first stage of adsorption (up to $\theta = 0.5$) involves a reconstructed surface in which oxygen atoms penetrate into the surface layer of the molybdenum. The Mo_2^+ behavior is consistent

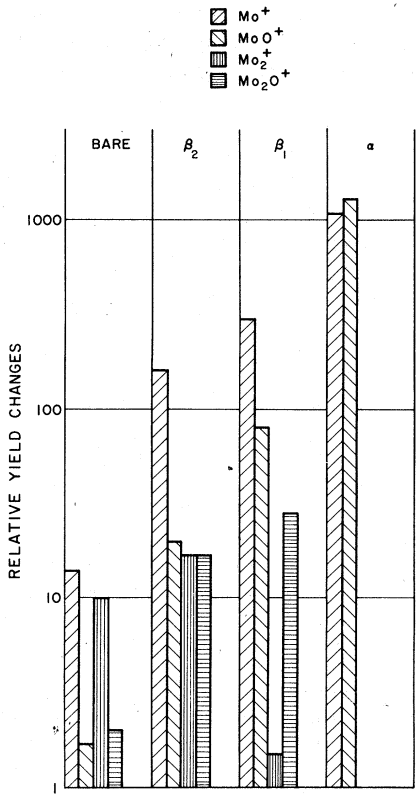

FIG. 18. Approximate changes in characteristic ion yields brought about by adsorption into the various α and β states at room temperature.

with this picture. In room-temperature adsorption, there is a steady progression in the kind of changes in ion yields as the β_2, β_1, and α states are filled. The α states are characterized by the ready production of MoO^+. MoO_2^+ seems to parallel MoO^+ but the yield is about ten times smaller. Exact details of Mo_2^+ and Mo_2O^+ behavior are masked by the beginnings of the oxide regime which suppresses their formation. Since the α states only form after substantial occupation of the β states, one might speculate in terms of some linear bonded entity filling spaces in the more tightly bound layer. However, knowledge of secondary-ion production mechanisms is still too limited to justify such interpretations in any detail. It is worthwhile reexamining the data on the transformation of the α_2 state indicated by the low-temperature loss of O_e^+ (Figs. 8 and 9). The transformation produces a small drop in MoO^+ but there are also small increases in Mo_2^+ and Mo_2O^+. The Mo^+ peak is almost unchanged. On refilling the α_2 state the Mo^+ and MoO^+ increase to higher levels for the same O_e^+ signal. These changes support the view that the process is a transformation rather than a loss, and that it is a transformation to a more strongly bound state.

The ionization patterns shown in Fig. 18 raise a number of questions concerning the mechanisms which control the secondary-ion yields. The most intriguing one is the very great influence of the α states on the total ion yield when the population of the α and β states is probably about equal.[16] Measurements of the electronic structure of the surface during oxygen desorption would provide an interesting comparison. As pointed out previously,[7] although the work function may be a significant parameter, it is not the dominant one since ion yields increase during oxidation even when the work function decreases.

E. Secondary-ion energies

The differences between the secondary-ion energy distributions for various species (Fig. 16) show the same trends as those in the work on titanium. It is interesting that, except for energy shifts apparently due to the work-function changes of the target, the distributions remain similar even though ion yields are changing by one or two orders of magnitude. Various simple models have been proposed[7] for secondary-ion production at clean surfaces, usually in terms of processes which give a velocity dependence of the ratio of ions to neutrals during sputtering. Different models propose different forms of velocity dependence. From the results presented here, whatever the mechanism which induces the increase in secondary-ion yields during oxygen adsorption, it does not involve a strong velocity-dependent factor. Furthermore, there is no marked temperature dependence of the secondary-ion energy distributions. Any theory of secondary-ion production must take account of these characteristics.

V. CONCLUSIONS

The study of oxygen adsorption on polycrystalline molybdenum at various temperatures using SIMS and EID has indicated that: (a) Oxygen chemisorbed on polycrystalline molybdenum at room temperature exists in two types of states, β and α. The adsorption regime is followed by an oxide regime. The α states are only populated after the β states are substantially occupied. (b) There are two β states with heats of adsorption of ~120 and 170 kcal/mole. (c) The α state is characterized by a heat of adsorption of 37 kcal/mole and a τ_0 of $10^{-5.7}$ sec. (d) There are two α states, one giving rise to electron-induced desorption of O_e^+ but the other not. (e) When the α states are only partially occupied at room temperature, there is a rapid transformation of the O_e^+ producing state on heating to >500 °K with an activation energy of roughly 7 kcal/mole. (f) The α states are associa-

ted with the ready production of MoO^+ secondary ions. For the β states, Mo_2O^+ production is more significant. (g) The structures responsible for MoO^+ and O_e^+ production are "locked" in place by the presence of the oxide regime. (h) At room temperature, both the α and β states fill at an initial rate equivalent to "monolayer" formation after about 3.3×10^{14} collisions/cm^2. (i) The variations in ion yield produced by each state of adsorption are linear at low coverage for each state. The α adsorption produces a much larger change in secondary-ion yields. (j) In favorable cases SIMS can be used to examine different states of adsorption and the kinetics of adsorption and desorption.

ACKNOWLEDGMENTS

I am deeply indebted to P. A. Redhead for some very helpful discussions throughout this work. I thank G. W. Richardson for his assistance with the operation of the experimental system.

[1]A. Benninghoven, Surf. Sci. 28, 541 (1971).
[2]A. Muller and A. Benninghoven, Surf. Sci. 41, 493 (1974).
[3]A. Muller and A. Benninghoven, Surf. Sci. 39, 427 (1973).
[4]A. Benninghoven, Z. Phys. 230, 403 (1970).
[5]P. H. Dawson, Surf. Sci. 57, 229 (1976).
[6]P. H. Dawson and P. A. Redhead, Rev. Sci. Instrum. 48, 159 (1977).
[7]P. H. Dawson, Surf. Sci. (to be published).
[8]M. Barber and J. C. Vickerman, Chem. Phys. Lett. 26, 277 (1974).
[9]M. Barber, J. C. Vickerman, and J. Wolstenholme, J. Chem. Soc. Faraday Trans. 1 72, 40 (1976).
[10]P. A. Redhead, Can. J. Phys. 42, 886 (1964).
[11]D. Lichtman and T. R. Kirst, Phys. Rev. Lett. 20, 7 (1966).
[12]A. Klopfer, Surf. Sci. 20, 129 (1970).
[13]K. Hayek, H. E. Farnsworth, and R. L. Park, Surf. Sci. 10, 429 (1968).
[14]H. K. Khan and S. Feuerstein, J. Chem. Phys. 50, 3618 (1969).
[15]G. J. Dooley and T. W. Haas, J. Vac. Sci. Technol. 7, 49 (1970).
[16]R. Riwan, C. Guillot, and J. Paigne, Surf. Sci. 47, 183 (1975).
[17]Y. Ballu and J. LeCante, Jpn. J. Appl. Suppl. 2, 249 (1974).
[18]P. H. Dawson, Int. J. Mass Spectrom. Ion Phys. 17, 447 (1975).
[19]W. L. Fite, Rev. Sci. Instrum. 47, 326 (1976).
[20]P. H. Dawson, in *Quadrupole Mass Spectrometry and Its Applications*, edited by P. H. Dawson (Elsevier, Amsterdam, 1976).
[21]P. A. Redhead (private communication).
[22]L. A. Petermann, Nuovo Cimento Suppl. 5, 364 (1967).
[23]P. H. Dawson, Proceedings of the Seventh International Mass Spectrometry Conference, Florence, 1976 (unpublished).